DEVELOPMENT OF A TWO-PARAMETER SEISMIC INTENSITY MEASURE AND PROBABILISTIC ASSESSMENT PROCEDURE

Paul P. Cordova[1], Gregory G. Deierlein[2], Sameh S.F. Mehanny[3], and C.A. Cornell[4]

ABSTRACT

A method to evaluate the seismic collapse performance of frame structures is presented, considering uncertainties in both the ground motion hazard and inelastic structural response to extreme input ground motions. The procedure includes a new seismic-intensity scaling index that accounts for period softening and thereby reduces the large record-to-record variability typically observed in inelastic time-history analyses. Equations are developed to combine results from inelastic time history analyses and a site-specific hazard curve to calculate the mean annual probability of a structure exceeding its collapse limit state.

1. INTRODUCTION

Research on performance-based earthquake engineering poses many challenges, among them being the need for a consistent methodology to predict structural collapse as a function of the earthquake ground motion intensity. Components to an assessment methodology for collapse should include (1) definition of the seismic hazard, (2) simulation of structural response to input ground motions, including stiffness and strength degradation, and (3) statistical interpretation of results. The methodology must rigorously account for variability in performance prediction arising due to uncertainties in the inherent seismic hazard and the nonlinear simulation of structural response.

A large source of variability in seismic performance assessment arises from simplifications in defining earthquake intensity relative to the true damaging effects of ground motions on structures. Current codes in the United States, such as the *International Building Code* (ICC 2000), define earthquake hazard in terms of spectral response coefficients, typically spectral acceleration measured at the first mode period of vibration, $S_a(T_1)$. First mode spectral acceleration is the basis of equivalent lateral force design procedures, and it is often used as the default earthquake intensity scaling parameter for time-history analyses. While first mode

[1] *Research Assistant, John A. Blume Earthquake Engineering Center, Stanford Univ., Stanford, CA 94305-4020*
[2] *Prof., Dept. of Civil & Env.l Engrg., Stanford Univ., Stanford, CA 94305-4020, email: ggd@stanford.edu*
[3] *Simpson Gumpertz and Heger, Inc., San Francisco, CA., email: SSFMehanny@sgh.com*
[4] *Prof., Dept. of Civil & Env.l Engrg., Stanford Univ., Stanford, CA 94305-4020, email: cornell@ce.stanford.edu*

spectral acceleration is an accurate index for structures that respond elastically, this single parameter does not reflect many of the aspects of earthquake ground motions that affect inelastic stiffness and strength degradation. An objective of this paper is to examine a new two-parameter hazard intensity index that can improve the accuracy of structural performance predictions based on inelastic time history analyses. A related objective is the development of reliability-based equations for interpreting the performance limit state to compare the effect of using a single versus two-parameter intensity measure.

The scope and approach of this paper is as follows. First, the general concepts of earthquake ground motion intensity measures are introduced, including an overview of traditional measures and the development of attenuation functions for the new proposed index. Second, a series of case study buildings are introduced and analyzed to determine their collapse limit state using incremented inelastic time-history analyses coupled with a post-earthquake stability analysis. Results of the case study analyses are used to calibrate the new earthquake intensity measure. Next, a probability-based assessment procedure is developed to describe the collapse performance in terms of mean annual probability of exceedance and an equivalent load and resistance format. Finally, the probabilistic assessment procedure is demonstrated through an application to one of the case study buildings.

2. HAZARD INTENSITY MEASURES

Traditionally, building codes have quantified earthquake intensity as a function of either peak ground motions (acceleration or velocity) or linear response spectrum quantities (acceleration, velocity, or displacement). As implied by their name, linear response spectrum quantities do a good job at characterizing earthquake effects in structures that respond elastically, but they do not necessarily capture inelastic behavior. More elaborate indices, which seek to improve characterization of earthquake ground motions, have been the subject of continuing studies. For example, Housner (1975) proposed combining spectral acceleration together with strong motion duration. More recently, Luco (2001) has proposed extending linear spectral quantities into the nonlinear realm through the use of inelastic spectral response demands. While they are generally more accurate, one drawback of the nonlinear spectral values is that they imply a coupling between the earthquake hazard definition and the inelastic structural properties. This complicates

development of seismic hazard maps for general use. Another topic of recent research concerns near fault directivity effects and whether these warrant specialized treatment in earthquake hazard characterization (e.g., Alavi & Krawinkler 2000). These are just a few examples of research to investigate the damaging features of earthquake ground motions and develop improved hazard intensity measures to represent these effects.

Common to most studies of improved intensity measures is the goal to characterize ground motion hazards in a statistically meaningful way for predicting structural performance. This implies that the best intensity measures are those that result in the least record-to-record variability, measured with respect to a common intensity index, when evaluating structural performance to multiple earthquake records. Of course, even with the best ground motion characterization, uncertainties will persist in characterizing the geologic earthquake hazard and in simulating inelastic structural performance.

Improved Hazard Intensity Measure - $S_a(T_1)R_{Sa}^{\alpha}$

The *International Building Code* (ICC 2000) and most other earthquake engineering design standards in the United States define hazard intensity as the spectral acceleration of the ground motion, typically calculated at the fundamental (first mode) period of the structure. A known shortcoming of this measure is that it does not account for inelastic lengthening of the period as the structure softens under stiffness degradation. As illustrated in the response spectra plots of Fig. 1, two ground motions characterized on the basis of their first-mode spectral response may result in significantly different inelastic response, depending on the slope of the spectra at lengthened periods. For example, when normalized with respect to $S_a(T_1)$, record #2 will inevitably produce larger inelastic deformations than record #1. This trend is not accounted for in the single spectral quantity, $S_a(T_1)$.

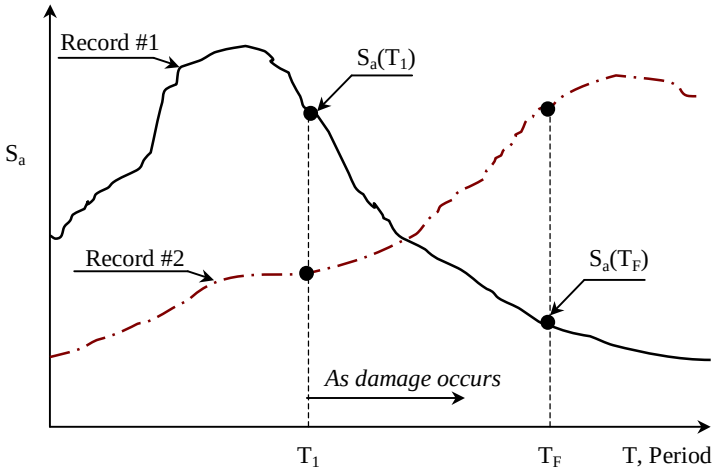

Figure 1 – Effects of structural softening.

A simple extension to current practice that can help capture the period shift effect is to introduce a second intensity parameter that reflects spectral shape. The proposed parameter to do this is a ratio of spectral accelerations at two periods,

$$R_{S_a} = S_a(T_f) \Big/ S_a(T_1) \quad (1)$$

where T_1 is the first mode period and T_f is a longer period that represents the inelastic (damaged) structure. This ratio can then be combined with the first mode spectral acceleration, $S_a(T_1)$, to give the following new two-parameter hazard intensity measure

$$S^* = S_a(T_1) R_{S_a}{}^{\alpha} \quad (2)$$

where α and the ratio T_f/T_1 are determined by calibration to optimize the intensity index by minimizing the variability in computed results.

Attenuation Functions for Two-Parameter Index

Given the prevalence of linear spectral acceleration in codes and practice, most hazard assessment techniques and data are geared toward this predicting this quantity. For example, national hazard maps available from USGS define earthquake hazard in terms of spectral acceleration at two periods (roughly *T = 0.2* second and *1* second) representative of short and long period structures. In devising new intensity measures, it is convenient if they can be derived by manipulating existing models and hazard data.

Since the proposed intensity measure, S^*, is simply a function of the spectral acceleration at two different periods (T_1 and T_f), it is relatively straightforward to modify existing attenuation function to accommodate this index. Equations 3 and 4 show the transformation of a single parameter attenuation function, $E[\ln S_a(T_x)]$, to the modified function, $E[\ln S^*]$, where $E[\ln \ldots]$ is read as the "expected value of the natural log of the given parameter" and other variables are as defined previously:

$$\ln S^* = (1-\alpha)\ln S_a(T_1) + \alpha \ln S_a(T_f) \quad (3)$$

$$E\left[\ln S^*\right] = (1-\alpha)E\left[\ln S_a(T_1)\right] + \alpha E\left[\ln S_a(T_f)\right] \quad (4)$$

In addition to the expected value of S^*, the standard deviation, $\sigma_{\ln S^*}$, must also be defined. This in turn requires the correlation between spectral accelerations at the two periods, $S_a(T_1)$ and

$S_a(T_f)$. Inoue (1990) provides the following empirical correlation coefficient, $\rho_{\ln Sa_1 \ln Sa_f}$, that fills this need:

$$\rho_{\ln Sa_1 \ln Sa_f} = 1 - 0.33\left|\ln(1/T_1) - \ln(1/T_f)\right| \quad (5)$$

Given this correlation expression, the standard deviation of *S** can be defined as follows:

$$\sigma^2_{\ln S^*} = (1-\alpha)^2 \sigma^2_{\ln Sa_1} + \alpha^2 \sigma^2_{\ln Sa_f} + 2\rho_{\ln Sa_1 \ln Sa_f}(1-\alpha)\alpha\sigma_{\ln Sa_1}\sigma_{\ln Sa_f} \quad (6)$$

Most spectral attenuation relationships define empirical coefficients as a function of frequency or period that can be manipulated to calculate *S** according to Eq. 4. For example, Abrahamson & Silva (1997) define an attenuation function as follows:

$$E[\ln S_a] = a_1 + a_4(m\text{-}m_1) + a_{12}(8.5\text{-}m)^n + [a_3 + a_{13}(m\text{-}m_1)]\ln(R) \quad (7)$$

where the *a*-coefficients are tabulated by Abrahamsom & Silva, *m* is the earthquake magnitude, m_1 is a given base magnitude, and *R* is the distance from the epicenter to the site. Substituting Eq. 7 into Eq. 4, one obtains the following relationship for modified coefficients that can be applied in the otherwise standard attenuation relationship to obtain *S*:*

$$a_x^* = (1-\alpha)a_{xT1} + \alpha a_{xT2} \quad (8)$$

These new relationships can then be applied in a standard probabilistic site hazard analysis where the required performance is evaluated on the basis of this new intensity, *S**.

3. BUILDING TESTBEDS

In related research (Mehanny et al., 2000, 2001) several moment frame structures have been developed and analyzed to exercise seismic assessment and design provisions for composite construction. These frames are utilized here to provide the basis for calibrating the new intensity measure parameters, α and T_f/T_1, and illustrate their application in a probabilistic performance assessment. The case study structures consist of three six-story frames and one twelve-story frame, all of which are designed according to provisions of the *International Building Code* (ICC 2000) and *AISC Seismic Provisions* (1997) for a site in a high seismic region of California. Due to space limitations the frames are only briefly introduced here. For further details the reader is referred to Mehanny et al. (2000, 2001).

Three of the case study structures are composite moment frames composed of reinforced concrete columns and steel beams (referred to as RCS systems), and the forth is a steel space frame. An elevation of one of the frames, a six-story RCS perimeter frame, is shown in Fig. 2. Beam sizes in the frames were generally governed by drift requirements while the reinforced columns were governed by the strong column weak beam criterion. As summarized in Table 1, vibration periods for the frames range from T_1 = 1.3 to 2.1 seconds (note – other data reported in Table 1 is discussed later).

Inelastic static and dynamic (time history) analyses are conducted using an analysis program developed by El-Tawil et al. (1996) that takes into account second-order geometric behavior and spread-of-plasticity effects in the beam-columns and connections. Inelastic component properties are based on the expected (as compared to nominal) material strengths, where the expected strengths are taken as 1.15 times the nominal strengths. Static pushover and inelastic time history analyses are run simultaneously with gravity loads equal to 100% dead load and 25% live load. Summarized in Table 1 are static lateral overstrengths of the frames, defined as $\Omega_o = V_u/V_d$ where V_u is the ultimate base shear and V_d is the IBC design base shear. The overstrengths range from roughly $\Omega_o = 2.6$ for the six-story RCS perimeter frame up to $\Omega_o = 6.1$ for the six-story steel space frame. The overstrengths are relatively large compared to the typical expected values of $\Omega_o = 2$ to 3, due to the following sources of overstrength: (1) expected versus minimum specified material strengths, (2) minimum stiffness (*drift*) criteria, (3) structural redundancy, (4) strong column criterion, and (5) discrete member sizing.

Table 1 – Testbed frame data

Frame ID	First Mode Period, T_1 (sec)	V_u/V_d, Ω	IDA Dispersion Data for Alternative Intensity Measures					
			General Records			Near Fault Records		
			$\sigma_{ln(IDR\|Sa)}$	$\sigma_{ln(IDR\|SaRsa)}$ (Optimized)	$\sigma_{lnIDR\|SaRsa}$ *(2.0,0.5)*	$\sigma_{ln(IDR\|Sa)}$	$\sigma_{ln(IDR\|SaRsa)}$ (Optimized)	$\sigma_{ln(IDR\|SaRsa)}$ *(2.0,0.5)*
6S_RCS_S	1.3sec	3.9	0.42	0.28 *(1.9,0.65)*	0.29	0.45	0.22 *(1.8,0.9)*	0.27
6S_S_S	1.3sec	6.1	0.27	0.20 *(1.2,2.4)*	0.23	0.30	0.18 *(1.6,0.8)*	0.19
12S_RCS_S	2.1sec	4.4	0.24	0.19 *(1.6,0.6)*	0.22	0.26	0.21 *(2.4,0.4)*	0.22
6S_RCS_P	1.5sec	2.6	0.30	0.23 *(1.65,0.45)*	0.24	-	-	-

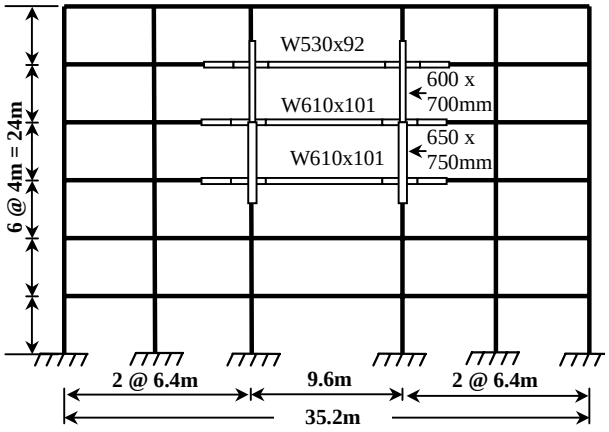

Figure 2 –Elevation of RCS perimeter frame.

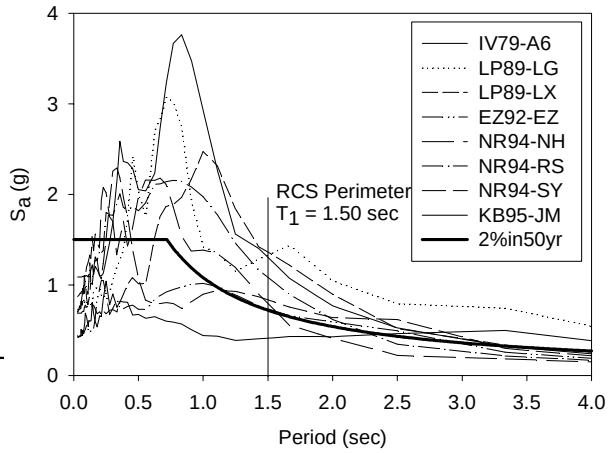

Figure 3 – Near Fault Response Spectrum

4. COLLAPSE ANALYSIS TECHNIQUES

Incremented Dynamic Analysis

Seismic performance is assessed through nonlinear time history analyses using two sets of ground motions – one comprised of eight general records and another of eight near-fault records with forward directivity. Response spectra for the near-fault records are superimposed on the 2% in 50-year design hazard spectrum used to design the case study buildings in Fig. 3. Acceleration components of the records are scaled, where the resulting ground motion intensity is reported in terms of either spectral acceleration, $S_a(T_1)$, or the proposed new index, $S_a R_{S_a}{}^{\alpha}$. Shome and Cornell (1997) have demonstrated that such scaling of records will not bias the results and is an appropriate technique for multi-level hazard analysis. More details on the ground record properties and scaling issues for the records are summarized by Mehanny (2000).

Results of the time history analyses are summarized by plotting the scaled intensity measure versus maximum Interstory Drift Ratio (IDR), creating what are referred to herein as Incremented Dynamic Analysis (IDA) curves. Shown in Fig. 4 are examples of the IDA curves for the RCS perimeter frame building subjected to the general records, where each data point corresponds to the peak IDR resulting from a single time history analysis. The collection of data points for a single ground record scaled to multiple hazard levels forms the IDA curve. Results are plotted in terms of the $S_a(T_1)$ intensity in Fig. 4a and $S_a R_{S_a}{}^{\alpha}$ in Fig. 4b.

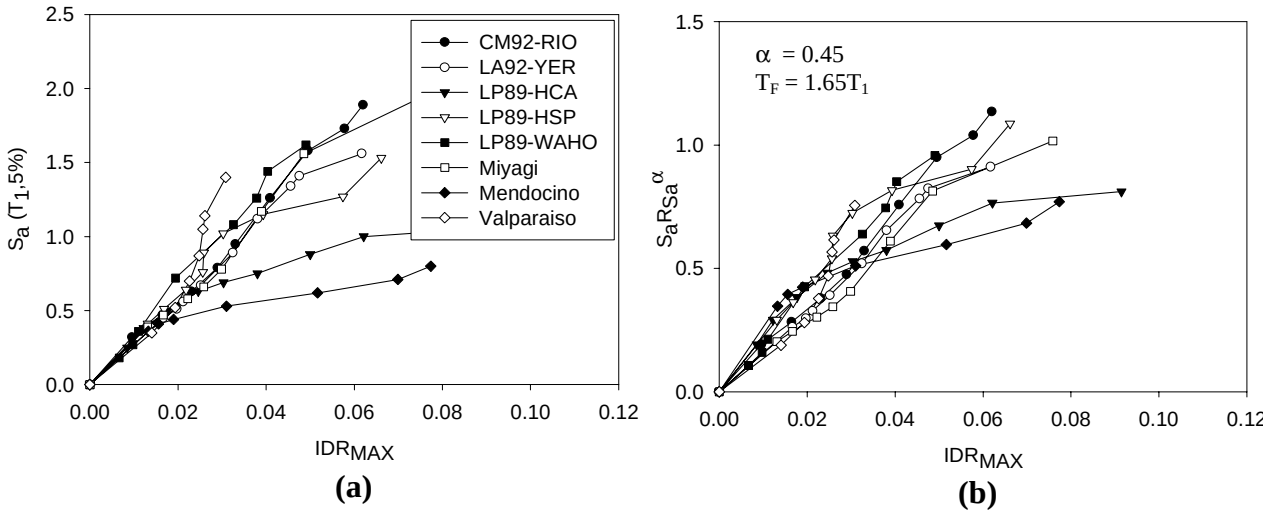

Figure 4 – IDA plots for 6S_RCS_P Frame: (a) IDR vs. $S_a(T_1)$ (b) IDR vs. $S_aR_{sa}^{\alpha}$

Comparing the graphs in Fig. 4, it is obvious that the two-parameter intensity measure (Fig. 4b) results in significantly less record-to-record variability than $S_a(T_1)$ (Fig. 4a). The variability can be quantified in terms of dispersion of the drift response conditioned on the ground motion intensity measure. Dispersion is calculated according to the following equation as the mean squared deviation of the drift data from an average response curve obtained by linear regression in log-log space between drift and the seismic intensity (of the form, ln $IDR_{MAX} = A + B$ ln IM):

$$\sigma_{\ln IDR_{MAX}|intensity\ measure} = \left[\sum_{i=1}^{n} (\ln IDR_{MAX,i} - \ln \hat{IDR}_{MAX})^2 \Big/ n-1 \right]^{\frac{1}{2}} \qquad (9)$$

where $IDR_{MAX,i}$ is the *i*th response calculated for a given intensity, $\hat{IDR}_{MAX}$ is the value from the regression curve, and *n* is the total number of observations (*n=8* in this case).

Comparing Figs. 4a and 4b, the dispersion $\sigma_{ln(IDR,Sa)}$ = 0.45 for the $S_a(T_1)$ index is roughly twice that of $\sigma_{ln(IDR,SaR)}$ = 0.22 for $S_aR_{S_a}^{\alpha}$. This result is based on using the optimized coefficients of $\alpha=0.45$ and $T_f/T_1 = 1.65$ for the $S_aR_{S_a}^{\alpha}$ index, determined by varying these factors so as to minimize the dispersion. Note that these optimal values are specific to the RCS six-story perimeter frame under the set of eight ground motions. Reduction in the dispersion in this way helps reduce the number of records necessary to simulate time history response within a specified confidence interval.

While the two-parameter index reduces the overall dispersion, this reduction is most apparent at larger drifts, where the structure behaves nonlinearly. In fact, comparing Figs. 4a and 4b, in the elastic range (at lower drifts), the two-parameter $S_a R_{S_a}{}^{\alpha}$ index results in more variability than *Sa(T_1).* This follows from the fact that *Sa(T_1)* provides a nearly exact correlation with drift for the linear case, whereas the period shift captured in $S_a R_{S_a}{}^{\alpha}$ works best when the structure behaves nonlinearly. This suggests that an improved index would be one where the α and T_f parameters are devised to vary with the degree of inelastic action, similar in some ways to how the period is shifted using the capacity spectrum method for calculating the target displacement for nonlinear static pushover analyses.

While the IDA's provides useful information on the structural response, it is apparent from the curves in Fig. 4 that the IDA's do not reveal a definitive stability limit state. Some curves, such as the one for the LP89-HCA record, asymptotically approach a bounding strength (in terms of the intensity measure), but others do not. For example, the CM92-RIO and Valparaiso plots maintain positive slopes at very large earthquake intensities and drifts. This reflects inherent limitations of the inelastic time-history analysis to fully capture the strength and stiffness degradation at large inelastic deformations.

Frame Stability Limit State Determination

To evaluate global instability, the authors have employed a procedure that integrates local damage indices, computed during the time-history analysis, through a supplementary stability analysis of the damaged structure. The basic procedure, described in detail by Mehanny and Deierlein (2001), entails a post-earthquake second-order inelastic stability analysis to assess the loss of gravity load capacity due to damage incurred during the earthquake. This procedure, which leads to the plot of an intensity measure versus gravity stability index λ_u shown in Fig. 5, entails three basic steps. (1) *Perform a nonlinear time-history analysis and calculate the cumulative damage indices.* This provides the basis to quantify the localized (distributed) damage caused by a given earthquake ground motion. The damage indices are empirical equations that track the structural damage as a function of cumulative plastic deformations. (2) *Modify the analysis model based on the damage incurred during the time-history analysis.* This

involves reducing element stiffness and strengths as a function of the cumulative damage indices and incorporating the residual (permanent) building drift into the structural topology. (3) *Reanalyze the modified structural model through a second-order inelastic static analysis under gravity loads up its inelastic stability limit*. The resulting stability index, λ_u in Fig. 5, is defined as the ratio of the vertical load capacity to the applied gravity loads, where the gravity loads are assumed as full dead load plus 25% of the live load.

The stability index, λ_u, provides a global failure criterion that integrates the effect of local damage sustained under each earthquake record and intensity. Figure 5 shows the evolution of the stability index for the six-story RCS space frame, where there is a one-to-one correspondence between stability points in Fig. 5 and the maximum interstory drifts in Fig. 4. The initial value of $\lambda_{uo} = 5.5$ (on the horizontal axis in Fig. 5) is the index for the undamaged structure, implying that the undamaged frame has sufficient lateral strength/stiffness to maintain stability under 5.5 times the gravity load. This large value reflects the fact that the structure has significant gravity-load overstrength as a result of the high seismic loads. The point where the curves cross $\lambda_u=1.0$ is point at which the structure can no longer sustain stability under its self-weight due to extensive seismic damage. The stability index at this point is defined as λ_f and the associated median value of the seismic hazard value is $\hat{\mu}_{\lambda_f}$. This level is defined as the 'capacity' – or collapse limit state – of the structure. Between these limits, λ_{uo} and λ_f, a third limit point is identified at $\lambda_u = 0.95\lambda_{uo}$, corresponding to the point at which the lateral stability begins to

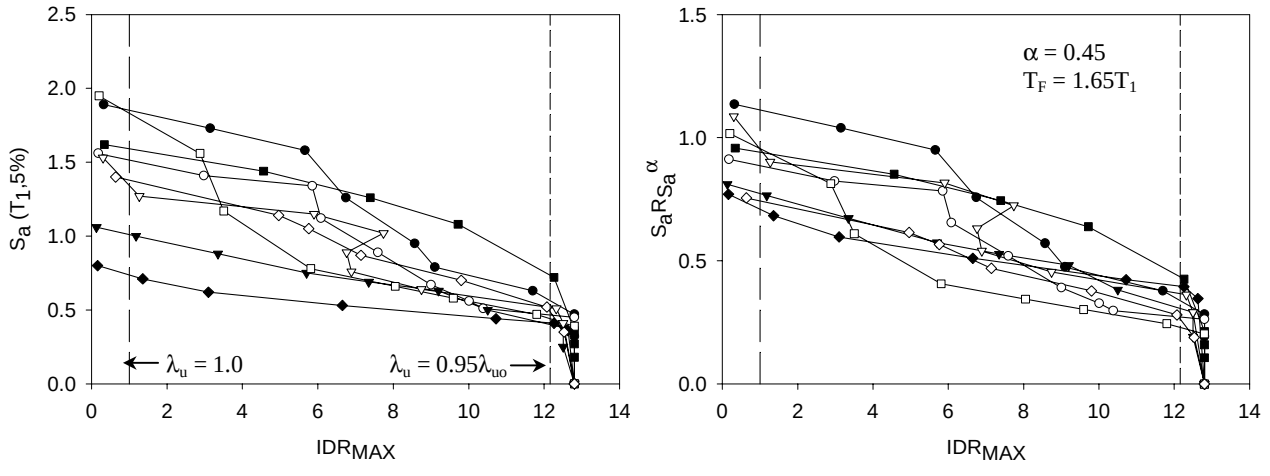

Figure 5 – Stability curves versus IM, (a) IM = S_a, (b) IM = $S_aR_{sa}^{\alpha}$

significantly degrade. This point, referred to as λ_{OD} (Onset of Damage) defines where there is a sharp transition in the $S_a(T_1)$ or $S_a R_{S_a}{}^{\alpha}$ versus λ_u stability curve, representing the intensity level beyond which the stability index degrades rapidly.

Similar to the IDA plots (Fig. 4), the $S_a(T_1)$ index shows much larger record-to-record variability in the λ_u response than the $S_a R_{S_a}{}^{\alpha}$ index. The standard deviations of $S_a(T_1)$ at λ_{OD} and λ_f are equal to 0.40 and 0.49, respectively, compared to 0.26 and 0.15 using $S_a R_{S_a}{}^{\alpha}$. This reduced variability leads to a better approximation of the expected collapse performance.

5. DETERMINATION OF GENERAL α AND T_f

The examples described above show how the proposed intensity measure, $S_a R_{S_a}{}^{\alpha}$, can significantly reduce the record-to-record variability in calculating the seismic performance. What remains to determine is optimum values of α and the period multiplier, $C=T_f/T_1$, which minimize dispersion for a broad class of building frames. To accomplish this, we will utilize analysis results of the four case study structures introduced previously.

To determine the optimal calibration for α and *C*, IDA and λ_u stability analyses are run for each of the four structures under the sixteen ground motions (eight general and eight near fault). Next, the $S_a R_{S_a}{}^{\alpha}$ response data is plotted for various combinations of α and *C*, the average response curve is fit to the data, and the dispersion is calculated. This results in many α and *C* pairs for each structure, each with its own dispersion, σ_{lnIDR}. The optimal α and *C* pair for each structure is one that yields the least dispersion. The graphs in Fig. 6 show the resulting relationships between α, *C*, and the resulting dispersion for each structure and bin of ground motions. The optimum alpha-coefficient is plotted versus the corresponding *C* in Fig. 6a, and the associated dispersions for the corresponding pairs of α and *C* are plotted in Fig. 6b.

Determination of one general pair of α and *C* obviously compromises the preciseness that can be achieved with multiple pairs tailored for each structure and each ground record. Nevertheless, a

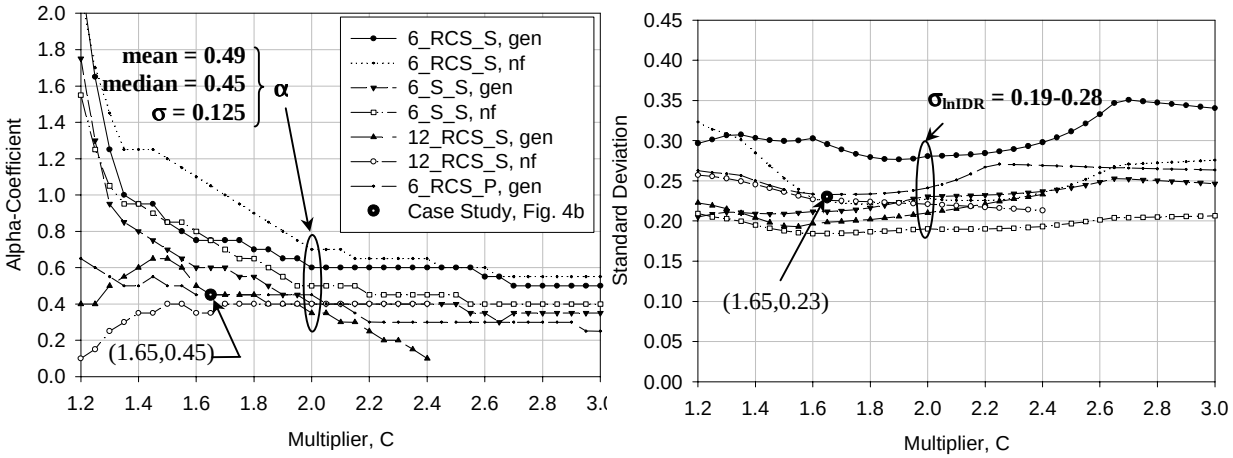

Figure 6 – Optimization of $S_aR_{Sa}^{\alpha}$, (a) Range of optimum α-C pairs and (b) Dispersion on α-C pairs.

common calibration is desired to make the procedure convenient for generalized use. Referring to Fig. 6b, on average the dispersion turns out to be relatively constant over a large range of *C* and α pairs. Further, from Fig. 6a we see that the optimal α (given *C*) is relatively stable for *2 < C < 3.* This indicates that the intensity measure is somewhat insensitive, within a certain range, to the choice of period multiplier. Based on these observations, a pair of *C = 2.0* ($T_f = 2.0T_1$) and α = 0.5 is proposed for general use. Thus, the proposed intensity measure takes the specific definition:

$$S^* = S_a(T_1)\left[S_a(2.0T_1) \Big/ S_a(T_1)\right]^{0.5} = S_a R_{S_a}{}^{0.5} \tag{10}$$

Based on this definition, the data in Figs. 4b and 5b are re-plotted and shown in Fig. 7. Dispersion data for all three intensity measures ($S_a(T_1)$, the optimal $S_aR_{S_a}{}^{\alpha}$, and the generalized $S_aR_{S_a}{}^{0.5}$) are summarized for each frame in Table 1.

Referring to Table 1, in all cases the proposed intensity measure *(SaR_{Sa}^{α})* consistently reduces the variability in the calculated structural response, compared to the *$Sa(T_1)$* index. The two-parameter index with optimum coefficients *(SaR_{Sa}^{α})* obviously does a better job than the average index ($SaR_{Sa}^{0.5}$ per Eq. 10), but the average index still does well – particularly where the dispersion is large for the original *$Sa(T_1)$* index. Conversely, the only cases where the new index fails to make a significant impact is those instances where the variability of the response is

already low when scaled by spectral acceleration alone. Comparing results for the average two-parameter index (Eq. 10) with $Sa(T_1)$, the two-parameter index reduces the range of dispersion from 0.24-0.45 for $Sa(T_1)$ to 0.19-0.29 for $SaR_{Sa}^{0.5}$.

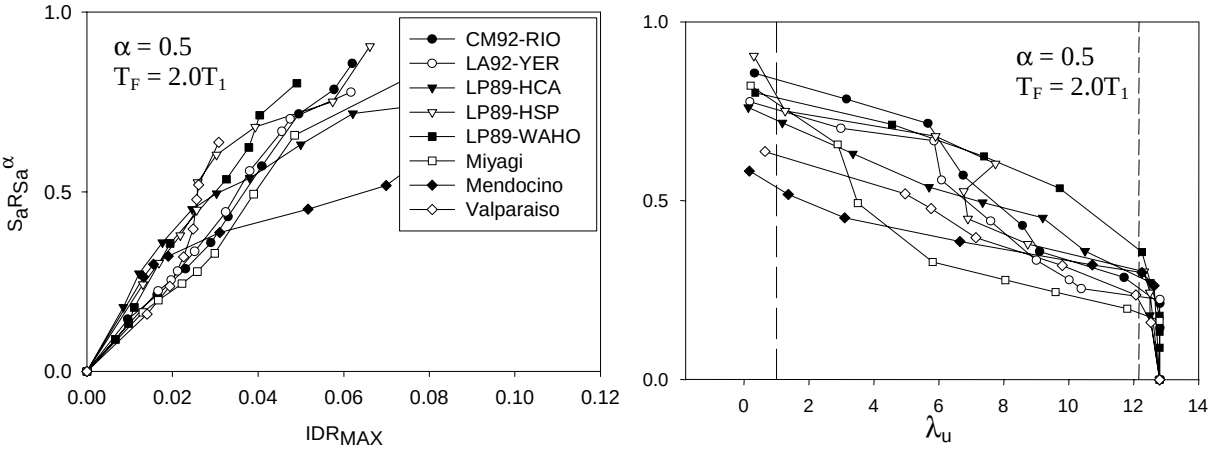

Figure 7 – Updated Behavior Curves with IM = $S_aR_{Sa}^{0.5}$
(a) IDA and (b) stability curves

6. PROBABILITY ASSESSMENT OF COLLAPSE PREVENTION

Using the inelastic time-history and stability analysis method described above, the "collapse prevention" performance for a given set of ground motion records is defined by the stability limit, $\hat{\mu}_{\lambda_f}$, defined in terms of the seismic hazard intensity – either $Sa(T_1)$ or $SaR_{Sa}^{0.5}$. The next step in the performance assessment is to compare the stability limit to the seismic hazard, considering the uncertainty in both the calculated response indices and the site hazard curve.

Mean Annual Probability of Exceedance

Defining failure (collapse) by the likelihood of the ground motion intensity exceeding the stability limit $\hat{\mu}_{\lambda_f}$ the mean annual probability of collapse can be described by the following:

$$P_f = P\left[IM \geq \hat{\mu}_{\lambda_f}\right] \tag{11}$$

Where P_f is the mean annual probability of failure and IM is the seismic hazard demand expressed using an intensity measure consistent with that used to define the stability limit, $\hat{\mu}_{\lambda_f}$. In this case, the two alternative intensity measures considered are $S_a(T_1)$ or $S_aR_{S_a}^{0.5}$. The

seismic demands are expressed in terms of a probabilistic hazard curve (the annual probability of exceeding a specified intensity measure), determined either explicitly by a probabilistic seismic hazard analysis or using published hazard maps.

Equation 11 can be further expanded into the following form using the total probability theorem:

$$P_f = \int_0^\infty H_{IM}(u)\, f_{\lambda_f}(u) du \tag{12}$$

Where u is the intensity measure, $H_{IM}(u)$ is the hazard curve, and $f_{\lambda_f}(u)$ is the probability density of the structural stability limit. To permit closed-form solution of the probability integral, the hazard function is assumed to take the following form:

$$H_{IM}(u) = k_o u^{-k} \tag{13}$$

where k_o and k are coefficients that fit Eq. 13 to the hazard data. Further, $f_{\lambda_f}(u)$ is assumed as a lognormal distribution with the median $\hat{\mu}_{\lambda_f}$ and the dispersion $\delta_{\lambda f}$ (or $\sigma_{ln(\lambda f)}$). Given these assumptions, the integral solution to Eq. 12 is as follows:

$$P_f = H_{IM}(\hat{\mu}_{\lambda_f}) e^{\frac{1}{2}k^2\delta_{\lambda_f}^2} \tag{14}$$

where $H_{IM}(\hat{\mu}_{\lambda_f})$ is the mean annual probability from the hazard curve evaluated at the median capacity $\hat{\mu}_{\lambda_f}$, and the other terms are as defined previously.

LRFD-like Format of Collapse Probability

An alternative way to envision the mean annual collapse probability is by rearranging Eq. 14 so as to compare the hazard demand to the structural capacity in a format similar to that used for *Load and Resistance Factor Design* (LRFD) provisions. Setting the failure probability in Eq. 14 to a maximum acceptance probability criteria, $P_f < P_{acceptance}$, Eq. 13 and 14 can be combined to give the design requirement:

$$k_o \hat{\mu}_{\lambda_f}^{-k} e^{\frac{1}{2}k^2\delta_{\lambda_f}^2} < P_{acceptance} \tag{15}$$

Rearranging this equation, the required capacity $\hat{\mu}_{\lambda_f}$ to ensure that the probability of failure is less than the acceptance criterion, $P_{acceptance}$, is given by the following:

$$\hat{\mu}_{\lambda_f} \geq IM_{P_{acceptance}} e^{\frac{1}{2}k\delta_{\lambda_f}^2} \tag{16}$$

where $IM_{P_{accep\,tan\,ce}}$ is the hazard intensity measure with the annual probability, $P_{acceptance}$, of being exceeded (i.e. $P_{acceptance} = H_{IM}(IM_{P_{acceptance}})$). The term, $e^{\frac{1}{2}k\delta^2_{\lambda_f}}$, which reflects the variability of the median stability limit $\hat{\mu}_{\lambda_f}$, can be moved to the left side of Eq. 16, resulting in the following:

$$e^{-\frac{1}{2}k\delta^2_{\lambda_f}}\,\hat{\mu}_{\lambda_f} \geq IM_{P_{acceptance}} \quad or \quad \phi\,\hat{\mu}_{\lambda_f} \geq \text{“seismic demand”} \tag{17}$$

where $\phi = e^{-\frac{1}{2}k\delta^2_{\lambda_f}}$. This equation is similar to LRFD equations that are prevalent in code provisions where the “design strength” on the left side (the nominal strength reduced by a phi factor) is compared to the load effect or “seismic demand”. In this case there is no load factor on the seismic demand since the recurrence interval of the demand is implicit in its definition.

An important but perhaps misleading coincidence in Eq. 17 is that the probability associated with the demand term (on the right side) turns out to be equal to the desired limit on the probability of exceeding the median stability intensity, $\hat{\mu}_{\lambda_f}$. This is different than saying that one is designing for a given hazard with a specified probability of exceedance. From Eq. 15, the underlying probability statement implied in Eq. 17 is related to the likelihood of exceeding the stability criterion, $\hat{\mu}_{\lambda_f}$ taking into account both variability in the ground motion hazard and the record-to-record variability in the stability index.

Essentially, Eq. 17 enables one to establish whether a structure meets the collapse performance objective with a mean annual probability of exceedance, $P_{acceptance}$. There are two basic input requirements for the procedure: (1) the “seismic demand” for the desired probability of exceedance, $IM_{P,acceptance}$, determined using either hazard maps or a probabilistic seismic hazard analysis; and (2) the median stability limit, $\hat{\mu}_{\lambda_f}$, of the structure and the corresponding dispersion δ_{λ_f} for a representative set of ground motions.

7. APPLICATION OF PROBABILISTIC COLLAPSE ASSESSMENT

This example will go through a collapse performance assessment for the 6-story RCS perimeter frame. The hazard analysis is based on a site at Yerba Buena Island (in San Francisco Bay)

where the San Andreas and Hayward faults govern the seismic hazard. The seismic hazard is characterized two ways: (1) through an explicit probabilistic seismic hazard analysis of the site and (2) using spectral acceleration hazard maps from building code provisions.

Annual Hazard Curves

Probabilistic Seismic Hazard Analysis (PSHA): Using the Abrahamson and Silva attenuation relationship presented in Eqs. 7 and 8, annual hazard curves for spectral acceleration, $S_a(T_1)$, and the proposed intensity measure, $S_a R_{S_a}{}^{0.5}$, can be developed through a standard probabilistic seismic hazard analysis for the Yerba-Buena Site site. Details of the hazard analysis are beyond the scope of this paper, but basically, this analysis provides a probabilistic assessment of earthquake magnitude and distance (M-R) pairs for the site, given its proximity to nearby faults.

Code Based Technique: An alternative (simplified) technique to obtain the hazard curve is to infer it from mapped spectral and site coefficients such as those provided by the seismic design provisions of the *International Building Code* (ICC 2000). The first step is to calculate the spectral acceleration for the site using the following equation:

$$S_a = F_v S_1 \Big/ T_1 \tag{18}$$

where F_v is a tabulated site coefficient, given as a function of the site (soil) class and the spectral coefficients, and S_1 is the spectral hazard coefficient obtained from seismic hazard maps with a an average probability of occurrence of 2% in 50-years. Implied by Eq. 18 is a 1/T spectral curve in the long period range. Using Eq. 18, one can directly obtain the 2% in 50 year (P_o = *0.0004*) spectral acceleration at the first mode period T_1, i.e., $S_a(T_1)$. One can also approximate the two-parameter index $S_a R_{S_a}{}^{0.5}$, by assuming that $R_{S_a} = 2 \left\langle = S_a(T_1)/S_a(2T_1) = 2T_1/T_1 \right\rangle$. Two approximations inherent in this assumption are that there is full correlation between the hazard values of $S_a(T_1)$ and $S_a(2T_1)$ and the *1/T* design spectrum accurately represents the hazard spectrum. Once the 2% in 50 year spectral values are known, the full hazard curve is constructed assuming $k = 4$, and then back-calculating the k_o parameter.

Hazard Curve Comparison: Hazard curves for $T_1 = 1.5$ seconds (the natural period for the six-story RCS perimeter frame) are shown in Fig. 8, and the corresponding hazard curve parameters

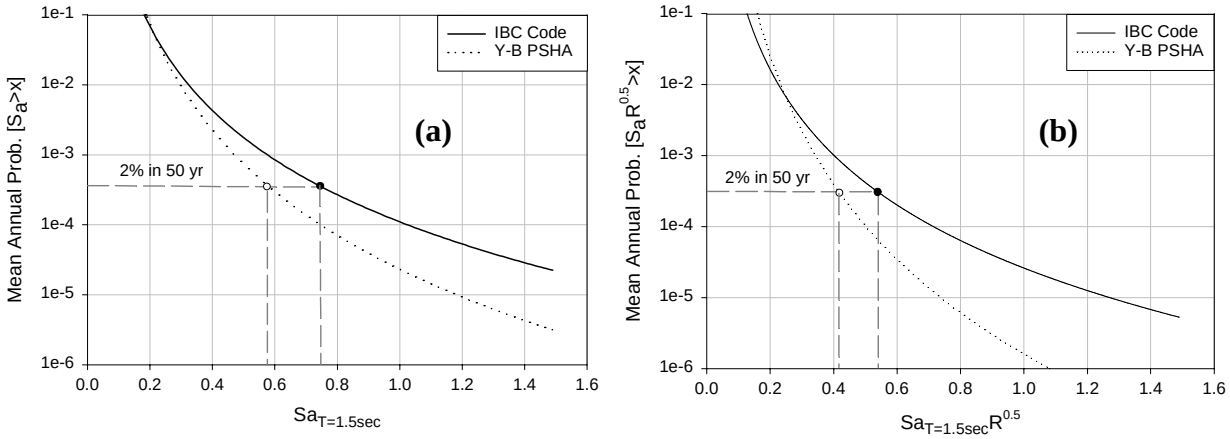

Figure 8 – Site Hazard Curves (a) S_a and (b) $S_aR^{0.5}$ (T_1 = 1.5 seconds)

are summarized in Table 2. Also summarized in Table 2 are capacity statistics $\hat{\mu}_{\lambda_f}$ and δ_{λ_f} for the frame. Referring to Fig. 8a, the 2% in 50 year value of $S_a(T_1)_{PSHA}$ = 0.57g from the probabilistic seismic hazard analysis is about 20% less than the code-value of $S_a(T_1)_{Code}$ = 0.72g, and there are corresponding differences over the entire hazard curve. Presumably the PSHA results are more accurate, but further studies would need to be done to confirm this. Referring to Fig. 8b, the difference between the PSHA and code approach at the 2% in 50 year level for the S_aR_{sa} index is also about 20%, $S_a(T_1)R^{0.5}_{Sa\ PSHA}$ = 0.40 versus $S_a(T_1)R^{0.5}_{Sa\ Code}$ = 0.51g.

Table 2 – Hazard curve coefficients and mean and dispersion of capacity

IM	Yerba Buena Site		Code Based Technique		$\hat{\mu}_{\lambda_f}$	δ_{λ_f}
	k_o	k	k_o	k		
$S_a(T_1)$	2.3×10^{-5}	5.0	1.1×10^{-4}	4	1.45	0.31
$S_aR_{Sa}^{0.5}$	1.6×10^{-6}	6.0	2.6×10^{-5}	4	0.76	0.15

Probability of Failure

Summarized in Table 2 are all the necessary data to compute the mean annual failure probabilities for the six-story RCS perimeter frame using the two alternative hazard intensity measures, $S_a(T_1)$ and $S_a(T_1)R^{0.5}_{Sa}$, and two alternative hazard curves (PSHA and building code approach). Substituting these data into Eqs. 13 and 14, the resulting collapse probabilities, P_f, are calculated and summarized in Table 3.

For the code hazard spectra and the $S_a(T_1)$ index, the mean annual probability of exceeding the stability (collapse) performance is about 0.00005 or roughly a 0.3% chance of exceedance in 50

years. Using the $S_a R_{S_a}^{0.5}$ index the probability roughly doubles to a mean annual value of 0.00009 or roughly a 0.5% in 50-year level. Since these probabilities are less than one-forth of the 2% in 50-year seismic hazard probability commonly used as the target for collapse prevention performance, these data suggest that current code provisions result in a conservative design for this case. Moreover, the failure probabilities are less by about a factor of five using the PSHA intensity data, implying an additional degree of conservatism in the design.

Another interesting question raised by the results in Table 3 concerns the different results obtained using the $S_a(T_1)$ versus $S_a R_{S_a}^{0.5}$ index. The fact that the two-parameter index results in higher failure probabilities suggests that for predicting collapse performance, simple scaling based on $S_a(T_1)$ may be unconservative. This follows from the logic that the two-parameter index more accurately represents the damaging effects of earthquakes in the hazard curve. Note, however, that the difference between the two indices is not too large for the Yerba Buena site analysis (PSHA) where the correlation between $S_a(T_1)$ and $S_a(T_f)$ is modeled more accurately than in the code-based technique.

Table 3 – Failure probability and capacity factor design factors

		Yerba Buena Site	Code Based Technique
Probability of Failure	$P_f(S_a(T_1))$	1.19 x 10^{-5}	5.37 x 10^{-5}
	$P_f(S_a R_{Sa}^{0.5})$	1.24 x 10^{-5}	9.29 x 10^{-5}
IM = $S_a(T_1)$	ϕ	0.78	0.82
	$\phi\mu_{\lambda f}$	1.13g	1.19g
	10%in50year	0.41g	0.48g
	2%in50year	0.56g	0.72g
IM = $S_a R_{S_a}^{0.5}$	ϕ	0.94	0.96
	$\phi\mu_{\lambda f}$	0.72g	0.73g
	10%in50year	0.30g	0.34g
	2%in50year	0.40g	0.51g

Factored Capacity versus Nominal Demand

An alternate way of assessing the analysis results is through the LRFD-like approach described by Eq. 17. Data for this method are summarized in the lower half of Table 3, where limiting values are reported for 2% in 50-year (0.0004) and 10% in 50-year (0.002) probability levels. Referring to Table 3, the ϕ factor ranges from $\phi = 0.78$ to 0.82 for the $S_a(T_1)$ index and from $\phi = 0.94$ to 0.96 for the $S_a R_{S_a}^{0.5}$ index. The large difference between these ranges is directly

related to the reduced dispersion achieved using the two-parameter $S_a R_{S_a}{}^{0.5}$ index as compared to the $S_a(T_1)$ index.

According to the criteria, $\phi\,\hat{\mu}_{\lambda_f} \geq IM_{P_{acceptance}}$, the frame collapse performance limit passes the 2% in 50-year and 10% in 50-year probability checks in all cases. These comparisons do reflect the relative difference in results between the $S_a(T_1)$ and $S_a R_{S_a}{}^{0.5}$ indices that is similar to the difference observed in the failure probabilities described previously. For example, consider the ratio $\phi\,\hat{\mu}_{\lambda_f} / IM_{P_{acceptance}}$ between the factored capacity and the hazard intensity. Using data from the Yerba-Buena PSHA at the 2% in 50-year level, the ratios are $\phi\,\hat{\mu}_{\lambda_f} / Sa_{2\%in50}$ = 1.13/0.56 = 2.0 for the $S_a(T_1)$ index and $\phi\,\hat{\mu}_{\lambda_f} / SaR_{Sa\,2\%in50}$ = 0.72/0.4 = 1.8 for the $S_a R_{S_a}{}^{0.5}$ index.

8. SUMMARY AND CONCLUSIONS

A method to assess seismic response and probabilistic collapse performance of structures is presented and demonstrated by application to a composite moment frame building. Included is a proposal for a new two-parameter earthquake hazard intensity measure $S_a R_{S_a}{}^{0.5}$ that reflects both spectral intensity and spectral shape, thus accounting for inelastic strength and stiffness degradation (period elongation). Data are presented which show that this proposed index significantly reduces the record-to-record variability in predicted response obtained from inelastic time history analyses. This has practical implications on improving the accuracy of seismic assessment methods and reducing the number of records necessary to obtain a given confidence in the results.

Equations are developed to interpret the probability of collapse using data from incremented dynamic analyses. The equations are presented in two formats, one that directly computes the probability of failure for a structure, and another, which mimics an LRFD format by applying a "phi-factor" to the capacity of the structure and comparing it to a specified hazard.

ACKNOWLEDGMENTS

This paper is based on research supported by the National Science Foundation (CMS-9632502 and CMS-9975501), the Pacific Earthquake Engineering Research center (NSF Award Number EEC-9701568), and Stanford University (graduate fellowship support for the first author).

REFERENCES

Abrahamson, N.A., and Silva, W.J. (1997), Empirical Response Spectral Attenuation Relations for Shallow Crustal Earthquakes, *Seismological Research Letters*, 68(1), 94-127.

AISC (1997), *Seismic Provisions for Structural Steel Buildings*, American Institute of Steel Construction, Chicago, IL

Alavi, B., Krawinkler, H. (2000), Consideration of Near-Fault Ground Motion Effects in Seismic Design, *Proc. of 12th World Conf. on Earthquake Engrg.*, New Zealand, 8 pg.

El-Tawil, S., and Deierlein, G.G. (1996), *Inelastic Dynamic Analysis of Mixed Steel-Concrete Space Frames*, Struct. Engrg. Report No. 96-5, Cornell Univ., Ithaca, NY.

Housner, G. W. (1975), Measures of severity of earthquake ground shaking, *Proceedings of the U.S. National Conference on Earthquake Engineering-1975*, Earthquake Engineering Research Inst., Oakland, California, June 1975, pages 25-33.

Inoue, T. (1990). Seismic Hazard Analysis of Multi-degree-of-freedom Structures, *Report No. RMS-8*, Stanford University, Stanford, CA.

ICC (2000), *International Building Code,* International Code Council, contact: BOCA, Country Club Hills, IL.

Luco, N. (2001), "Probabilistic Seismic Demand Analysis, SMRF Connection Fractures, and Near-Source Effects", Ph.D. Thesis, CEE Dept., Stanford Univ., Stanford, CA.

Mehanny, S.S., Deierlein, G.G. (2000), Modeling and Assessment of Seismic Performance of Composite Frames with Reinforced Concrete Columns and Steel Beams, *J.A. Blume Earthquake Engineering Center, Technical Report No. 135*, Stanford, CA.

Mehanny, S.S., Cordova, P.P., and Deierlein, G.G. (2001), Seismic Design of Composite Moment Frame Buildings – Case Studies and Code Implications, *Composite Construction IV*, ASCE, in press.

Mehanny, S.S., Deierlein, G.G. (2001), Seismic Damage and Collapse Assessment of Composite Moment Frames, *Jl. of Structural Engineering, 127(9),* ASCE, (to appear).

Shome, N., and Cornell, C.A. (1997), "Probabilistic Seismic Demand Analysis of Nonlinear Structures," *Report No. RMS-35*, Stanford University, Stanford, CA, 320 pgs.